

*Full Length Research Paper*

# Temperature compensation of hot wire mass air flow sensor by using fuzzy temperature compensation scheme

Noraznafulsima Khamshah<sup>1,2\*</sup>, Ahmed N. Abdalla<sup>2</sup>, Mohd Tarmizi Ibrahim<sup>1</sup>, Damhuji Rifai<sup>1</sup> and Shaiful Rizalme Wahid<sup>2</sup>

<sup>1</sup>Faculty of Electrical Automation Engineering Technology, TATIUC, Kemaman 24000, Terengganu, Malaysia.

<sup>2</sup>Faculty of Electrical and Electronic Engineering, University of Malaysia Pahang, Pekan 26300, Malaysia.

Accepted 11 June, 2012

Mass air flow sensors are increasingly used in the automotive industry to measure the mass air flow intake into the internal combustion engine. A problem occurred with the basic circuit for bridge type mass air flow sensor is the measurement accuracy of the sensor is affected by the temperature variation in the air. This paper presents the development of an open loop Fuzzy Temperature Compensation Scheme (FTCS) for hot wire mass air flow sensor. In order to verify the performance of the proposed scheme, first a simulation model was developed using Matlab/Simulink. Then, based on the Matlab/Simulink simulation, the FTCS has been implemented in hardware based real-time using Digital Signal Controllers, (dsPIC) with the Programming C Language. The effectiveness of the proposed fuzzy compensation scheme was verified with the estimation error within only 1% over the full-scale value.

**Key words:** Hot wire, mass air flow sensor, temperature compensation, fuzzy logic.

## INTRODUCTION

Thermal anemometry is still a widely used method for air velocity measurement in research and industry, in spite of the appearance of modern tools in recent decades. In thermal anemometry, the heat transfer from a heated wire placed in a fluid flow, measures the air velocity. If only the fluid velocity varies, then the heat loss can be interpreted as a measure of that variable. This sensor was operated under constant temperature or constant current conditions and also works for flow-rate measurements in a wide range of applications (Bradshaw, 1971; Hinze, 1975; Emrich, 1981; Bardakhanov, 2012). Its major applications are in moderate to high velocities under isothermal conditions such as wind tunnel measurements, but thermal anemometry can be adapted to a variety of applications in different fields. In automotive applications, hot wire is used in mass air flow sensor to measure the mass air flow intake into an internal combustion engine. This measurement is then used by the engine controller to

optimize the performance of the engine with regard to maximizing fuel efficiency. Thus, it is desirable then to have a mass air flow sensor which provides accurate and reliable results independently of air temperature. As the heat transfer process is sensitive both to the mass air flow and temperature of the air, any changes in temperature must be compensated for in order to achieve accurate mass air flow measurements. The hardware compensated schemes for temperature compensation of hot wire thermal flow sensor have been proposed by a few researchers (Drubka et al., 1977; Takagi, 1986; Lee et al., 1995; Ligeza, 1998; Nam et al., 2004; Sosna et al., 2010). However, there are some problems occurred in hardware compensation, and cannot achieve the requirements of high-accuracy test results measured.

This paper focus on issues of software compensated scheme for hot-wire mass air flow sensor based on computational intelligence, Sugeno-Type Fuzzy Inference System. The proposed Fuzzy Temperature Compensation Scheme incorporates intelligence into the mass air flow sensor system. The correction of ambient effects, such as temperature requires continuous

\*Corresponding author. E-mail: [azna0309@yahoo.com](mailto:azna0309@yahoo.com).

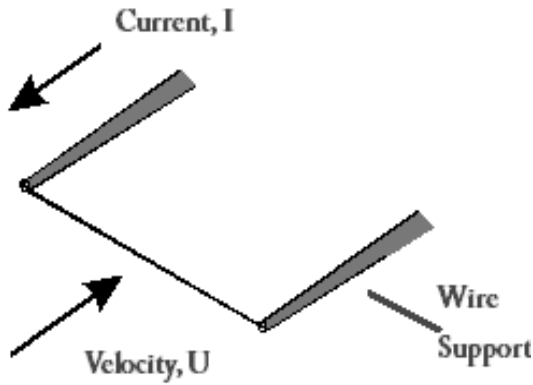


Figure 1. Hot wire anemometer.

monitoring and online correction of the sensor behavior. The effectiveness of the proposed fuzzy compensation scheme is verified both in simulation and experiment at different temperature variations. Performance comparison of the output voltage of the hot wire mass air flow sensor without compensates and after compensated is provided. These comparison results demonstrate the better improvement in the sensor measurement accuracy by reducing the percentage error caused by the temperature variations. Using on board memory, correction for temperature sensitivity is done in software, allowing sufficient improvement in accuracy compared to hardware trim techniques. A real time implementation of the proposed scheme is also described.

### Hot wire sensing principle

Fundamentally, a hot wire makes use of the principle of heat transfer from a heated surface being dependent upon the flow conditions passing over it. Hot wire anemometer consists of a thin wire mounted to supports and exposed to a velocity  $U_{as}$  as shown in Figure 1. When current is passed through a wire, heat is generated. In equilibrium, this must be balanced by heat loss (primarily convective) to the surroundings. If velocity changes, the convective heat transfer coefficient will change, wire temperature will change and eventually reach a new equilibrium. The most common wire materials are tungsten, platinum and a platinum-iridium alloy. A thin platinum coating is usually applied to improve bond with the plated ends and the support needles. The needles should be thin but strong and have high thermal resistance (low thermal conductivity) to the probe body (Fraden, 2010).

As the fluid or air passes over the hot wire, it carries away heat. The heat loss depends on the flow rate, the heat capacity of the fluid, and the temperature difference between the wire and the fluid/air. Since the heat capacity of the fluid is known, and the temperatures are monitored in real-time, the flow rate can be determined from the heat loss related to the electrical resistance of the wire via the (Ohm's law), and the temperature coefficient of the wire (Melani et al., 2008).

The differential equation that describes the temperature of the single wire is as follow:

$$\rho_w c_w A_w \frac{\delta T_w}{\delta t} = \frac{I^2 \chi_w}{A_w} - \pi d_w h (T_w - T_a) \quad (1)$$

The resistance of the sensor element can be approximated as a linear function of temperature, that is:

$$R_w = R_a [1 + \alpha_a (T_w - T_a)] \quad (2)$$

Typical representatives of this subclass of thermal flow sensors are hot wire and hot-film anemometers (Perry, 1982; Lomas, 1986). In constant temperature type hot wire, the temperature is maintained constant at any reasonable flow rate of the increase in supplying electric power. That power is the measure of the flow rate. In a CTA hot wire, the wire has a positive temperature coefficient and thus is used for a dual purpose; to elevate temperature above the media temperature (so it will be a cooling effect), and also to measure that temperature because the wire resistance goes down when the wire cools (Fraden, 2010). Figure 2 shows a simplified bridge circuit for the constant temperature method.

The feedback from a servo amplifier keeps the bridge in a balanced state. Resistor  $R_1$ - $R_3$  are constant, while  $R_w$  represents the resistance of the hot wire and is temperature dependent. Drop in the wire temperature,  $T_w$  causes a temporary drop in  $R_w$  and a subsequent reduction in the bridge voltage  $-e$  that is applied to the negative input of the servo amplifier. This leads to increase in  $V_{out}$ , which is applied to the bridge as a feedback. When  $V_{out}$  goes up, current  $I$  through the wire increase, leading to increase in temperature. This restores the wire temperature when flowing media attempt to cool it, so  $T_w$  remains constant over the entire flow rate range. The feedback voltage  $V_{out}$ , is the output signal of the circuit and the measure of the mass flow rate. The output voltage becomes higher according to the flow. Under a steady flow rate, the electric power  $Q_e$  supplied to the wire is balanced by the out-flowing thermal power  $Q_T$ , carried by the flowing media due to a convective heat transfer. That is,

$$Q_e = Q_T \quad (3)$$

Considering the heating current  $I$ , the wire temperature  $T_w$ , temperature of the fluid  $T_a$ , the wire surface area  $A_w$ , and the heat transfer coefficient  $h$ , the balance equation is:

$$I^2 R_w = h A_w (T_w - T_a) \quad (4)$$

King (1914) developed a solution of a heat loss from an infinite cylindrical body in an incompressible low Reynolds number flow:

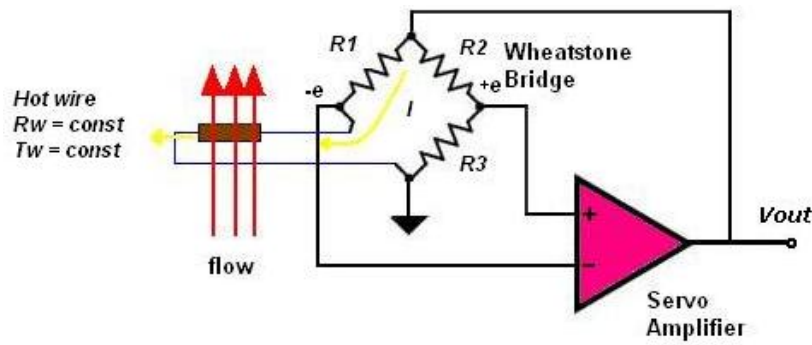


Figure 2. CTA hot wire anemometer with bridge.

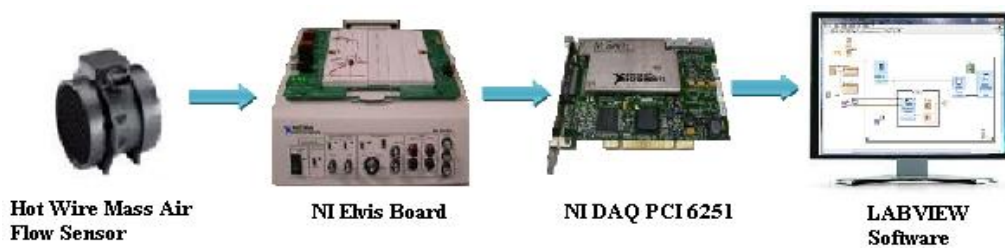


Figure 3. Schematic diagram of measurement setup.

$$h = a + bv_f^c \tag{5}$$

Where a, and b, are constant and  $c \approx 0.5$ .

This equation is known as the King’s Law. Combining the above three equations allows eliminating the heat transfer coefficient  $h$ :

$$a + bv_f^c = \frac{I^2 R_w}{A_w (T_w - T_a)} \tag{6}$$

Considering that,

$$V_{out} = i(R_w + R_1) \tag{7}$$

Then, the equation for the output voltage as a function of the mass flow rate is:

$$V_{out} = (R_w + R_1) \sqrt{\frac{A_w (a + b\sqrt{v})(T_w - T_a)}{R_w}} \tag{8}$$

**Accuracy and error analysis**

The schematic diagram of the measurement setup is shown in Figure 3. Six differential flows were applied to the hot wire mass flow sensor. The temperature has

been varied from 50 to 100°C to study the output voltage of the sensor. In this research, the 50°C was selected as the standard temperature. The output voltage of the hot wire, MAF Sensor was sent to the PC through a data acquisition (DAQ) device for data recording, data post-processing and measurement display. The serial interfacing for DAQ are using the NI-DAQ PCI 6251 and NI-Elvis Board, while the data collection and logging was done by using LABVIEW Software.

The averages for sampling data have been calculated to get the output voltage at each temperature variation. The output voltage versus mass air flow graph for the variation of temperature has been developed as shown in Figure 4. The output voltage for the hot wire sensor measurement is changing with the variation of temperature and affected the accuracy of the sensor measurement.

Based on selected standard temperature, the absolute error of measurement is as in Equation 10:

$$e_i = V_{T_i} - V_{50^\circ C} \tag{9}$$

Where,  $V_{T_i}$  is the voltage measured at the temperature  $T_i$  and  $V_{50^\circ}$  is the voltage measured at standard temperature. According to that, the percentage error in the measurement is:

$$\%e_i = \frac{V_{T_i} - V_{50^\circ c}}{V_{50^\circ c}} \tag{10}$$

According to the collected data, the absolute error and percentage of error for each output voltage have been

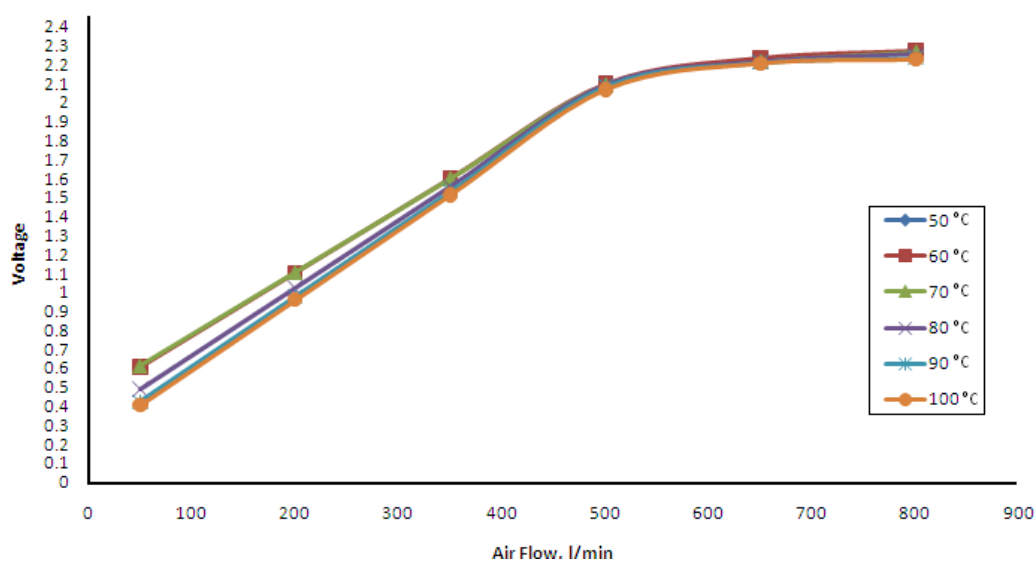


Figure 4. Variation of output voltage with different temperature.

calculated to measure the offset value of measurement compared to standard value. The absolute error at the different temperatures is used. The standard temperature, 50°C is set to standard zero. The data of the empirical errors at the different temperatures from 60 to 100°C for different flow rate of air and absolute error and percentage error are shown in Table 1. The experimental data showed that the error becomes higher with the temperature increasing.

#### FUZZY TEMPERATURE COMPENSATION SCHEME

Based on the empirical result of accuracy and error analysis of the mass flow rate in Table 1, the sensor should be compensated in such a way that its offset voltage due to its variation of ambient temperature from the standard temperature would be minimized. Thus, the sensor output is independent of temperature in the working range. For that purpose, a temperature compensation scheme has been proposed by using the fuzzy inference system as shown in Figure 5. The proposed scheme enables the direct readout of the input physical parameters after measuring its value and its compensation for the change of temperature. Here, the actual sensor and fuzzy compensation scheme are connected in cascade. In this scheme, the sensor output is fed as the inputs of the scheme and the error is corrected based on the rules designed according to expert experience.

Fuzzy logic controllers are based on fuzzy set and fuzzy logic theory, which emerged as a consequence of the proposal of fuzzy set theory by Zadeh (1973). The basic block diagram of an FLC is shown in Figure 6.

The complete process of mapping from a given input to an output using fuzzy logic is known as fuzzy inference. There are two types of fuzzy inference methods namely Mamdani type and Sugeno type. The difference between the two methods is only the way their outputs are

defined. In Mamdani type FLC, output is defined by the centroid of a two-dimensional function. However, in the Sugeno type FLC, the output membership functions are only linear or constant singleton spikes. In Sugeno type inference, implication and aggregation methods are fixed and cannot be edited. The implication method is simply multiplication and the aggregation operator just includes all the singletons. Regardless of the type, a fuzzy inference is based on five steps, which are, pre-processing, fuzzification, fuzzy inference engine (rule base), defuzzification and post-processing.

The first step of a fuzzy inference system designed is to take inputs and find out the degree to which they belong to each of the appropriate fuzzy sets via membership functions. The process of converting a numerical variable, which is a real or crisp value, into a linguistic variable (fuzzy value) is called fuzzification. For this scheme, six linguistic variables have been developed according to the error values which are zero, small, med-small, medium, med-large and large. Each linguistic value is assigned a trapezoidal membership function as shown in Figure 7.

For this proposed scheme, the Sugeno-Type Fuzzy Inference is used. The six rules used for error correction in this proposed fuzzy system are as follows:

- If (input is TZ) then (output is zero)
- If (input is TS) then (output is small)
- If (input is TMS) then (output is med-small)
- If (input is TM) then (output is medium)
- If (input is TML) then (output is med-large)
- If (input is TL) then (output is large)

The individual rule based inference was used as it is

**Table 1.** Absolute error and percentage error of hot wire MAF Sensor measurement.

| Mass air flow<br>l/min | Standard value<br>50°C | Temperature variations |                    |                      |
|------------------------|------------------------|------------------------|--------------------|----------------------|
|                        |                        | Measured voltage, V    | Absolute error (e) | Percentage error (%) |
| <b>60°C</b>            |                        |                        |                    |                      |
| 50                     | 0.6093                 | 0.6065                 | 0.0028             | 0.4609               |
| 200                    | 1.1116                 | 1.1041                 | 0.0076             | 0.6800               |
| 350                    | 1.6139                 | 1.6016                 | 0.0123             | 0.7628               |
| 500                    | 2.1162                 | 2.0992                 | 0.0171             | 0.8062               |
| 650                    | 2.2418                 | 2.2357                 | 0.0062             | 0.2745               |
| 800                    | 2.2918                 | 2.2736                 | 0.0182             | 0.7963               |
| <b>70°C</b>            |                        |                        |                    |                      |
| 50                     | 0.6093                 | 0.6108                 | 0.0015             | 0.2422               |
| 200                    | 1.1116                 | 1.1043                 | 0.0074             | 0.6627               |
| 350                    | 1.6139                 | 1.5977                 | 0.0162             | 1.0043               |
| 500                    | 2.1162                 | 2.0912                 | 0.0251             | 1.1838               |
| 650                    | 2.2418                 | 2.2146                 | 0.0273             | 1.2161               |
| 800                    | 2.2918                 | 2.2646                 | 0.0273             | 1.1896               |
| <b>80°C</b>            |                        |                        |                    |                      |
| 50                     | 0.6093                 | 0.4883                 | 0.1211             | 19.8655              |
| 200                    | 1.1116                 | 1.0221                 | 0.0896             | 8.0590               |
| 350                    | 1.6139                 | 1.5558                 | 0.0581             | 3.6015               |
| 500                    | 2.1162                 | 2.0896                 | 0.0267             | 1.2599               |
| 650                    | 2.2418                 | 2.2130                 | 0.0288             | 1.2846               |
| 800                    | 2.2918                 | 2.2530                 | 0.0388             | 1.6929               |
| <b>90°C</b>            |                        |                        |                    |                      |
| 50                     | 0.6093                 | 0.4250                 | 0.1844             | 30.2568              |
| 200                    | 1.1116                 | 0.9786                 | 0.1330             | 11.9669              |
| 350                    | 1.6139                 | 1.5323                 | 0.0817             | 5.0615               |
| 500                    | 2.1162                 | 2.0859                 | 0.0303             | 1.4341               |
| 650                    | 2.2418                 | 2.2113                 | 0.0305             | 1.3611               |
| 800                    | 2.2918                 | 2.2343                 | 0.0575             | 2.5095               |
| <b>100°C</b>           |                        |                        |                    |                      |
| 50                     | 0.6093                 | 0.4062                 | 0.2032             | 33.3421              |
| 200                    | 1.1116                 | 0.9601                 | 0.1516             | 13.6338              |
| 350                    | 1.6139                 | 1.5140                 | 0.0999             | 6.1929               |
| 500                    | 2.1162                 | 2.0679                 | 0.0483             | 2.2842               |
| 650                    | 2.2418                 | 2.2064                 | 0.0354             | 1.5807               |
| 800                    | 2.2918                 | 2.2264                 | 0.0654             | 2.8553               |

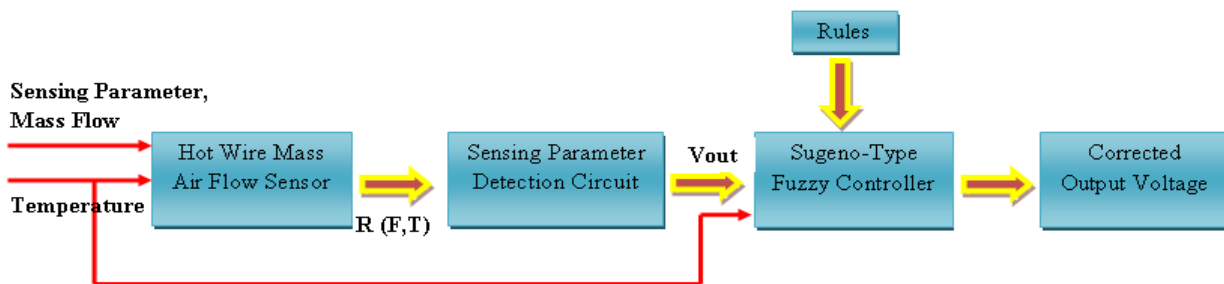


**Figure 5.** Scheme of Fuzzy Temperature Compensation.

computationally efficient and saves a lot of memory. In individual rule based inference, first each single rule was fired. This firing can be described as computing the

degree of the match between the crisp input and the fuzzy sets, describing the meaning of the rule antecedent, and clipping the fuzzy set describing the

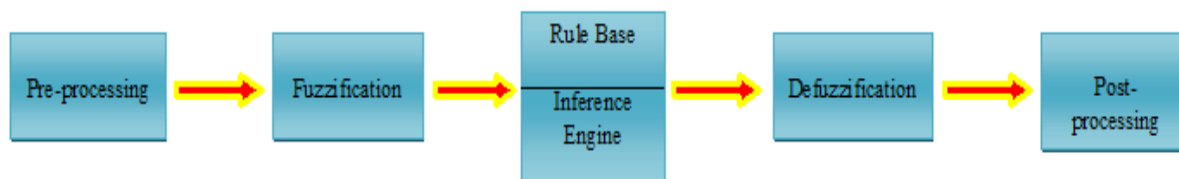


Figure 6. Basic block diagram of FLC.

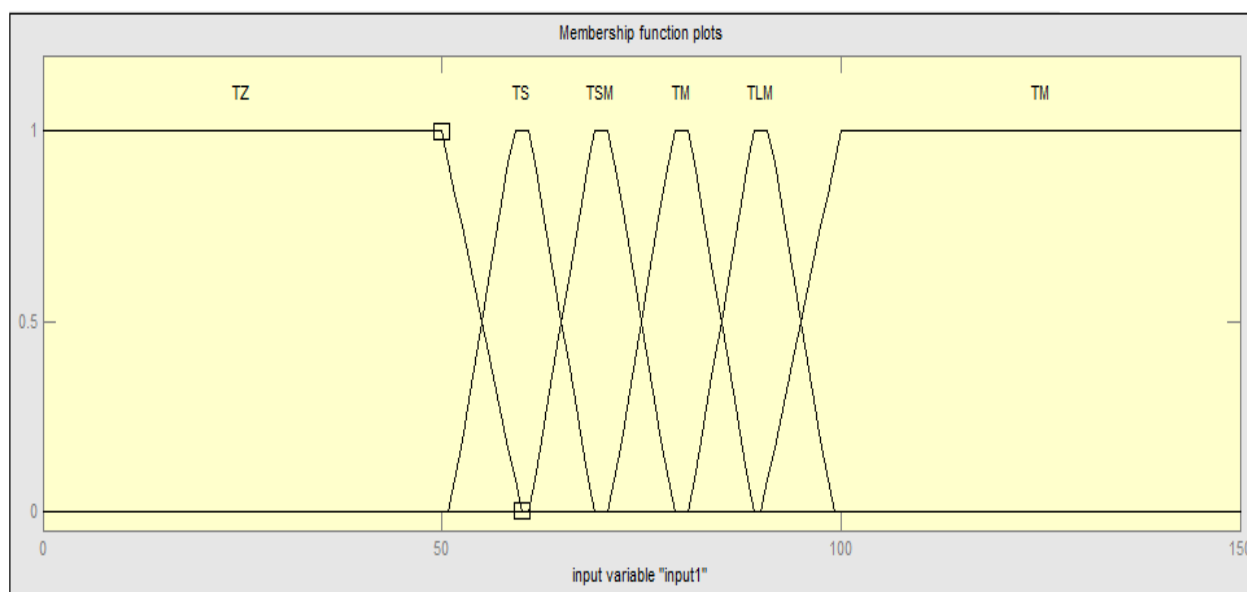


Figure 7. Input membership function.

meaning of the rule consequent on which the rule-antecedent has been matched by the crisp input. Finally, the clipped values for the control output of each rule are aggregated, which gives the value of the overall control output. The firing of rules based for this scheme is as shown in Figure 8. The FLC’s control surfaces are shown in Figure 9.

Defuzzification is the final step of fuzzy inference to obtain the control output. The center of gravity/area defuzzification method is the most popular among all the methods, and was used in this scheme. In this method, the crisp output value,  $x$  is the abscissa under the centre of gravity of the fuzzy set:

$$u = \frac{\sum_i \mu(x_i)x}{\sum_i \mu(x_i)} \tag{11}$$

Where,  $x_i$  is an operating point in a discrete universe and  $\mu(x_i)$  is its membership value of the membership function. This expression can be interpreted as the weighted average of the elements in the support set.

**Simulation studies**

The simulation studies have been carried out using

MATLAB/Simulink Toolbox. The Fuzzy temperature compensation scheme simulink model developed is shown in Figure 10.

The simulation result for uncompensated and compensated scheme is shown in Figure 11. From the figure, it is shown that the hot wire mass air flow sensor output have been compensated using the fuzzy temperature compensation scheme.

The simulation result for compensating voltage output at mass flow of 350 *l/min* have been chosen to demonstrate the performance of the fuzzy temperature compensation scheme. Figure 12 shows the temperature effect of compensating voltage output at different temperature corresponding to the desired mass flow of 350 *l/min*. Figure 13 shows the percentage error of the uncompensated and compensated output of fuzzy temperature compensation scheme model with the desired output. It is only within  $\pm 1\%$  of its full-scale value. It is a great improvement comparing -6.1% with the uncompensated voltage output as different temperature.

**Real-time implementation**

Based on the simulation studies result, the coding for designing a fuzzy temperature compensation scheme has been developed and embedded in dsPIC30F4013

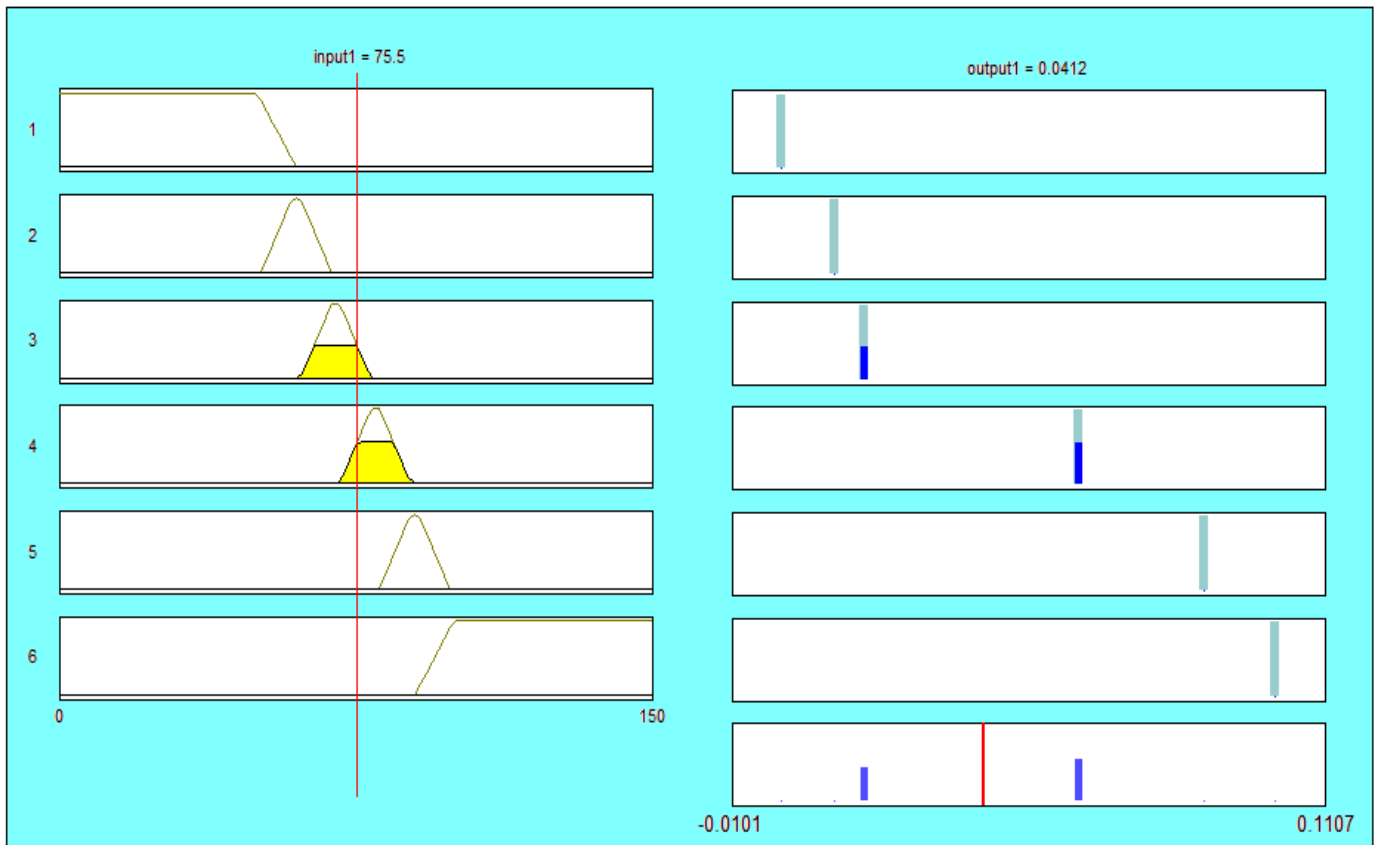


Figure 8. Firing of rule base.

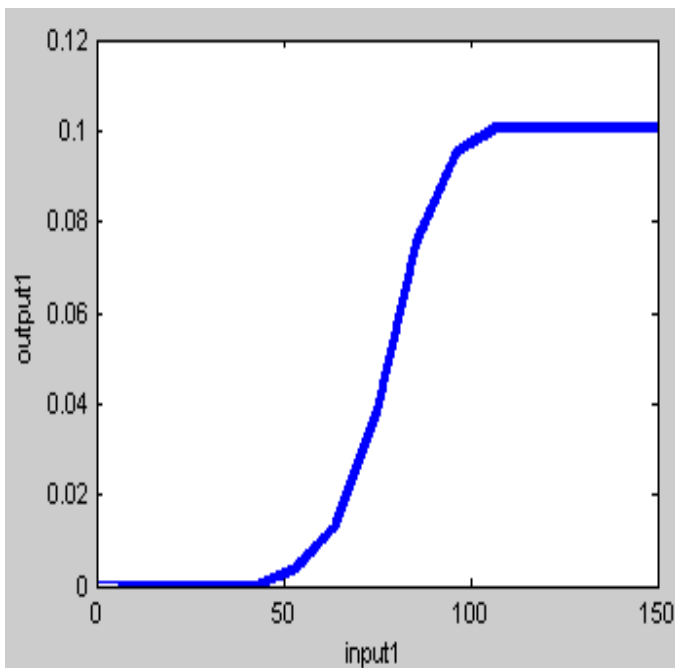


Figure 9. FLC's control surface.

with C Programming Language. The fuzzy coding for membership function is:

```

void cal_mf_lvl(unsigned short temp)
{
    unsigned char;
    unsigned long a,b;
    for(i=0;i<mf;i++)
    if(temp<=temp_mf[i][0])
    temp_lvl[i]=0;
    else if(temp<temp_mf[i][1])
    if((temp_mf[i][1]-temp_mf[i][0])==0)
    temp_lvl[i]=100;
    else
    a=temp_mf[i][1]-temp_mf[i][0];
    b=temp-temp_mf[i][0];
    temp_lvl[i]=(b*100)/a;
    else if (temp<=temp_mf[i][2])
    temp_lvl[i]=100;
    else if (temp<temp_mf[i][3])
    if((temp_mf[i][3]-temp_mf[i][2])==0)
    temp_lvl[i]=100;
    else
    a=temp_mf[i][3]-temp_mf[i][2];
    b=temp-temp_mf[i][2];
    temp_lvl[i]=100-((b*100)/a);
    else
    temp_lvl[i]=0;
}
    
```

While for rules are,

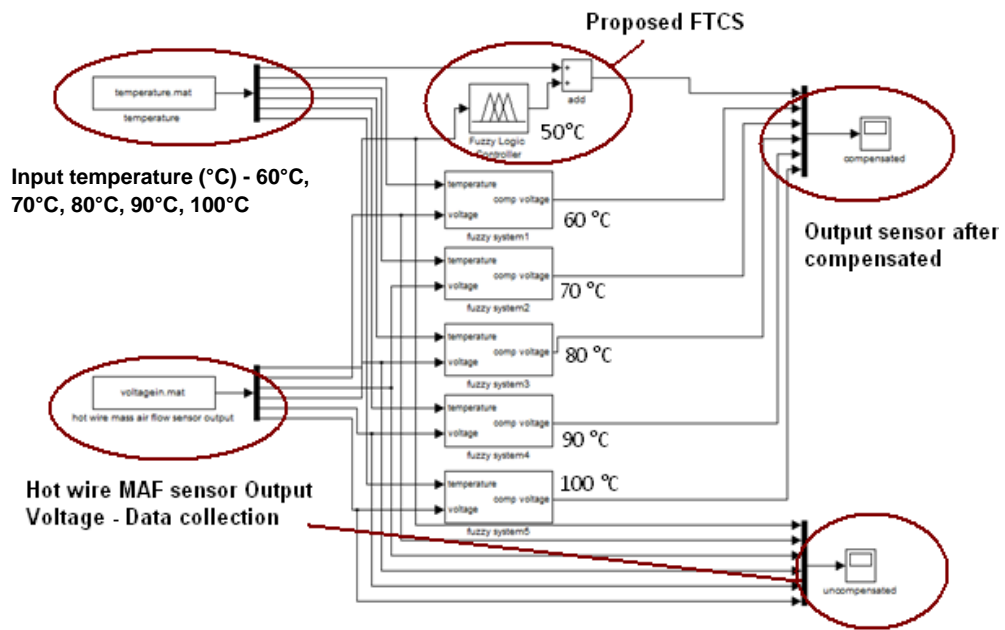


Figure 10. Fuzzy temperature compensation scheme simulink model.

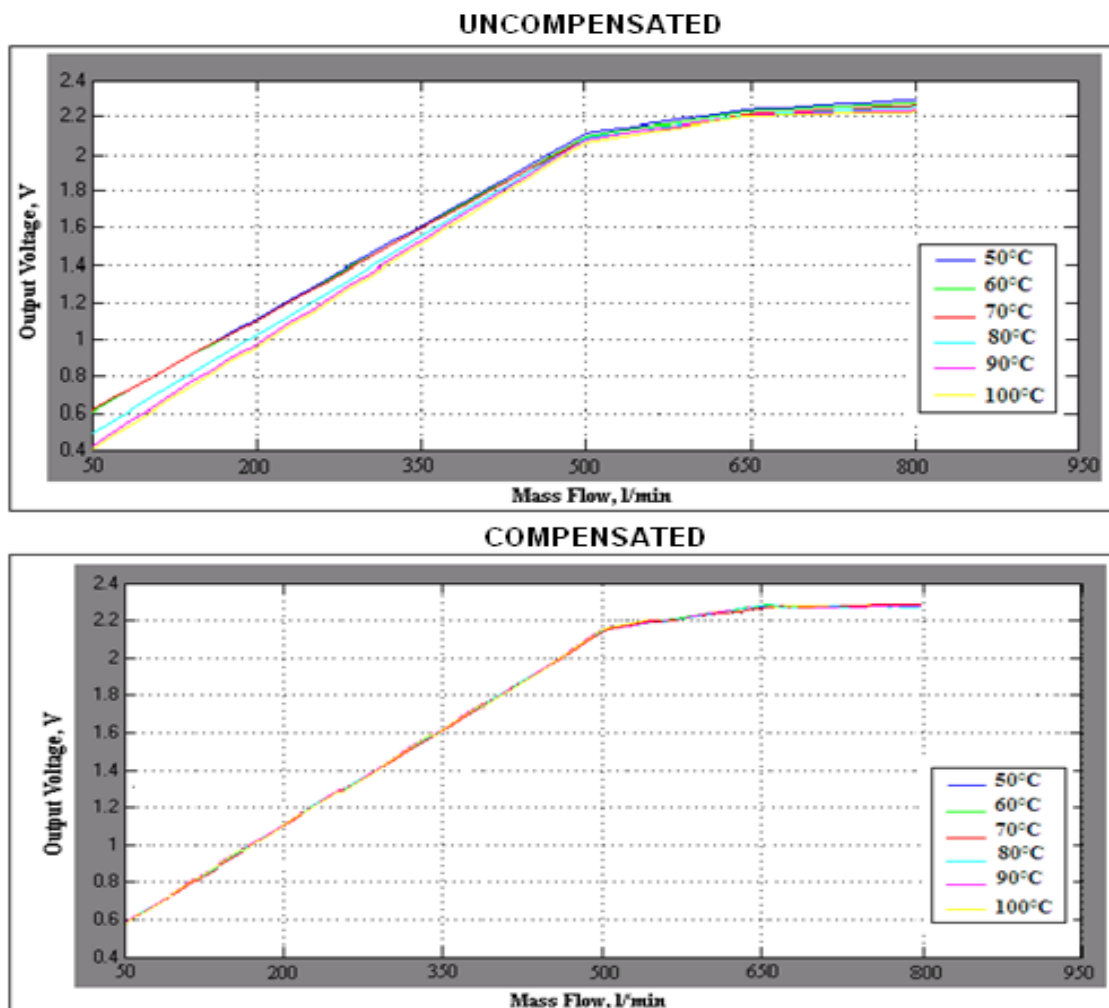


Figure 11. Simulation result for fuzzy temperature compensation scheme.

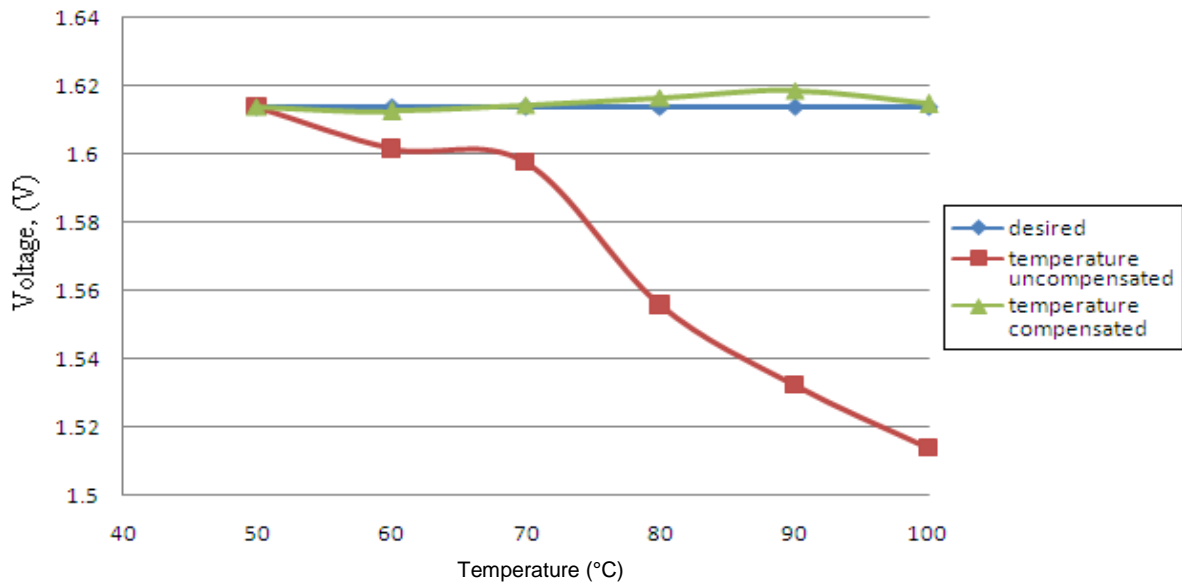


Figure 12. Temperature effect of compensating voltage output at different temperature for mass flow of 350 l/min.

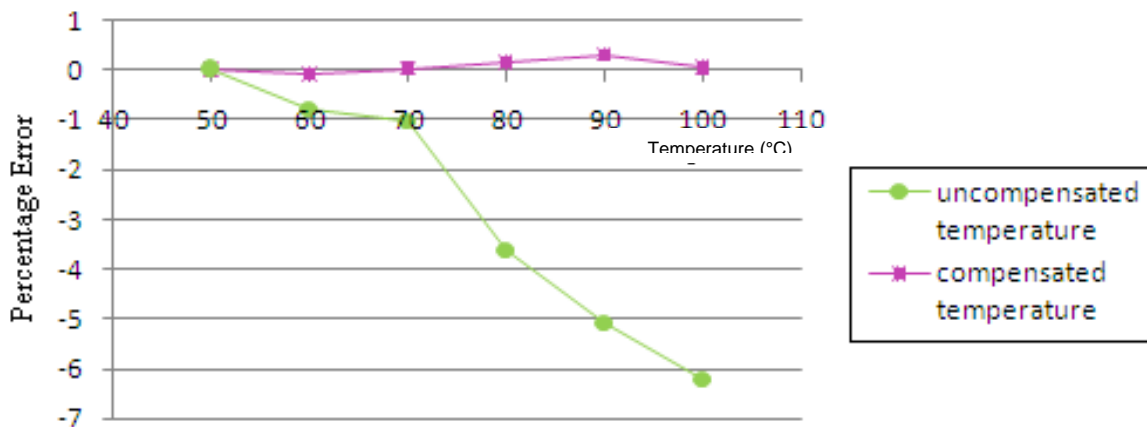


Figure 13. Percentage error of the uncompensated and compensated output for mass flow of 350 l/min.

```

if(rules[i][1]==zero)
if (templvl>=outmflevel[0])
outmflevel[0]=templvl;
else if(rules[i][1]==small)
if (templvl>=outmflevel[1])
outmflevel[1]=templvl;
else if(rules[i][1]==med_small)
if (templvl>=outmflevel[2])
outmflevel[2]=templvl;
else if(rules[i][1]==medium)
if (templvl>=outmflevel[3])
outmflevel[3]=templvl;
else if(rules[i][1]==med_large)
if(templvl>=outmflevel[4])
outmflevel[4]=templvl;
else if(rules[i][1]==large)
if (templvl>=outmflevel[5])
outmflevel[5]=templvl;
    
```

The dsPIC is used because it has larger RAM and higher

speed of instruction execution compared to PIC. The hardware for real implementation was constructed as shown in Figure 14.

The proposed scheme validation has been done by using real-time measurement of mass flow of 350 l/min. The output value after compensation and error correction has been displayed using LCD display as shown in Figure 15.

### Conclusion

This study describes a technique by using Sugeno-Type Fuzzy for compensating the significant error due to temperature variation in hot wire mass flow sensor for automotive application. The fuzzy temperature compensation scheme has been utilized to compensate the effect of temperature on the sensor characteristics over a temperature range from 60 to 100°C. It is shown that the estimation error of the scheme was within ±1%

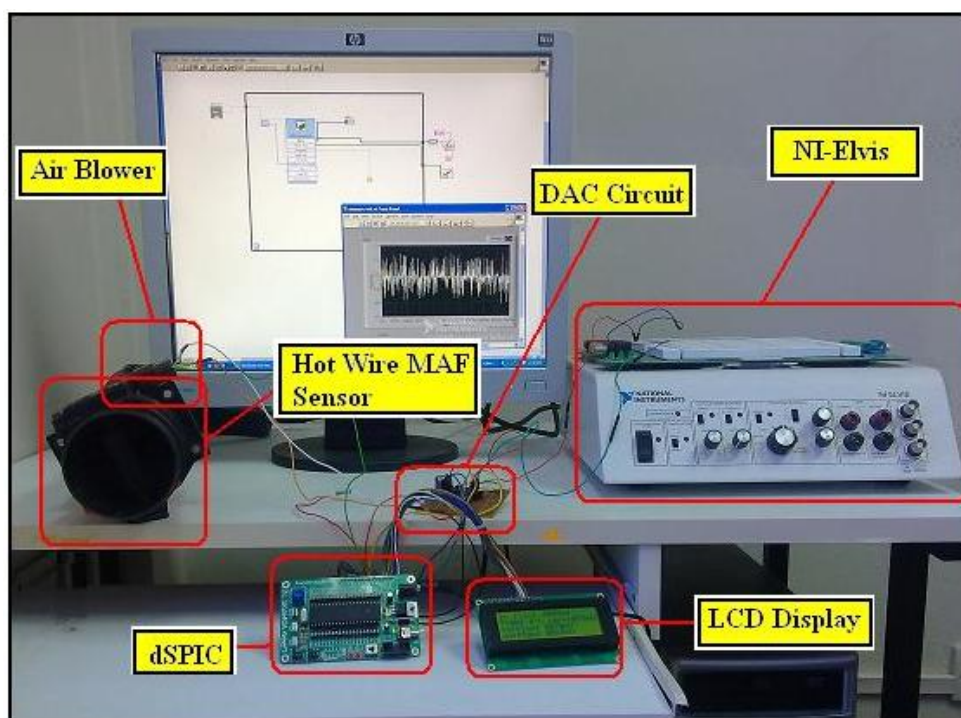


**Figure 14.** Real-time implementation of fuzzy temperature compensation scheme.

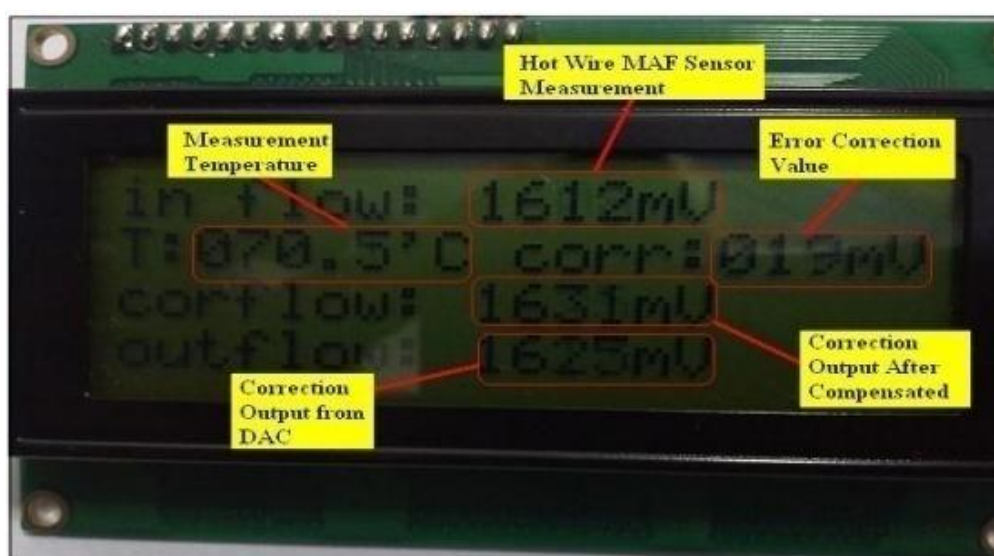


**Figure 15.** LCD Display for mass flow of 350 l/min.

over its full-scale value. The hardware for real-time implementation of the scheme using the digital signal controller (dsPIC) is presented. The proposed scheme was embedded in a dsPIC chip by using C Programming Language, and the output voltage achieved the desired temperature compensation. In future, hot wire mass air flow sensor temperature compensation's research could be extended into other intelligent technique areas in order to increase its applicability. For example, for the hardware temperature compensation, the Particle Swarm

Optimization (PSO) method can be used to identify and optimized the parameters involve in hot wire mass air flow sensor. Instead of that, software compensation also could use another intelligent method such as Genetic Algorithm (GA) or Ant Colony.

#### ACKNOWLEDGEMENT

This research was supported by the TATI University

College (Short Grant 9001-9002) and University Malaysia Pahang.

#### REFERENCES

- Bardakhanov SP, Lysenko VI, Trafanor DY (2012). Use of hot-wire anemometry for measuring the nanopowder. Springerlink J. Fluid Dyn. 47(2):281-287
- Bradshaw P (1971). An Introduction to Turbulence and its Measurement. Oxford, Pergamon Press.
- Drubka RE, Tan-atichat J, Nagib HM (1977). Analysis of Temperature Compensating Circuits for Hot-wires and Hot-films. DISA Inform. 22:5-14.
- Emrich RJ (1981). Methods of Experimental Physics. Academic Press. New York.
- Fraden J (2010). Handbook of Modern Sensors: Physics, Designs, and Applications.
- Lee SP, Kim JI, Kauh S (1995). Temperature Compensation of hot-wire anemometer with photoconductive cell. Exp. Fluids 19(5):362-365.
- Ligeza P (1998). A modified temperature-compensation circuit for CTA. Meas. Sci. Technol. 9(3):452-457.
- Lomas CG (1986). Fundamentals of Hot Wire Anemometry. Cambridge, Cambridge University Press.
- Melani M, Bertini L, Marinis MD, Lange P (2008). Hot Wire Anemometric MEMS Sensor for Water Flow Monitoring. Design, Automation, and Test in Europe, ACM New York, USA.
- Nam T, Kim S, Park S (2004). The temperature compensation of a thermal flow sensor by changing the slope and the ratio of resistances. Sens. Actuat.-A. 114:212-218.
- Perry AE (1982). Hot-Wire Anemometry. Oxford, UK, Oxford University Press.
- Sosna C, Buchner R, Lang W (2010). A Temperature Compensation Circuit for Thermal Flow Sensors Operated in Constant-Temperature-Difference Mode. Instrum. Meas. IEEE Trans. 59(6):1715-1721.
- Takagi S (1986). A hot-wire anemometer compensated for ambient temperature variations. J. Phys. E: Sci. Instrum. 3:452-457.
- Zadeh LA (1973). Outline of a new approach to the analysis of complex system and decision processes. IEEE Trans. Syst. Man Cyber 3:28-44.